Engineering with Computers (2021) 37:3771–3791
https://doi.org/10.1007/s00366-020-01027-6

ORIGINAL ARTICLE

Inverse structural damage identification problem in CFRP laminated plates using SFO algorithm based on strain fields

Guilherme Ferreira Gomes[1] · Fabricio Alves de Almeida[2] · Antonio Carlos Ancelotti Jr.[1] · Sebastião Simões da Cunha Jr.[1]

Received: 22 July 2019 / Accepted: 18 April 2020 / Published online: 14 May 2020

Abstract
Damage detection methods are an important field of engineering and crucial in terms of structural safety. However, in many practical cases, the process of monitoring and identifying damage is extremely difficult or even impractical due to the conditions of access and operation of a given component/structure. In this study, an inverse algorithm based on strain fields for damage identification in composite plate structures is presented. The inverse analyses combine experimental tests and digital image correlation (DIC) with numerical models based on finite element update method with great advantage of being a non-contact method. The proposed technique identifies the location and dimension of damages in a CFRP plate using static strains formulated as an objective function to be minimized. By model updating, the discrepancies between the experimental and the numerical results are minimized. For the success of the model updating, the efficiency of the optimization algorithm is essential. A powerful new metaheuristic sunflower optimization (SFO) is employed to update the unknown model parameters. Experimental results showed the excellent efficiency in the combined use of DIC, numerical modeling and SFO optimization to accurately identify the location of damage in numerical and experimental tests. The obtained results indicate that the proposed method can be used to determine efficiently the location and dimension of structural damages in mechanical structures.

Keywords Structural health monitoring · Inverse problem · Sunflower optimization · Digital image correlation · Composite plates

1 Introduction

The detection of damages is a field of extreme importance in engineering, since through it corrective maintenance can be applied and in this way structural safety can be guaranteed. A prognosis of the structure can be made from the moment that a damage is correctly detected, thus being able to evaluate the integrity of the structure and determine its life time [1, 2].

In the same way, the application of composite materials has become increasingly constant in several areas of industry, but especially in the aerospace field. Its use is justified due to the fact that this type of material has good mechanical characteristics such as high stiffness, high mechanical strength and stiffness-to-mass ratio [3–5].

At the same time, despite these good mechanical characteristics, composite materials can present certain failures when subjected to extreme conditions such as static overload, impact, fatigue, design errors and overheating [6, 7]. These faults can be translated as matrix microcracking, interface delamination and then a strength redistribution followed by fiber rupture [8, 9]. Most of the methods used to detect damage are currently visual or experimental, such as acoustic or ultrasonic methods, thermography, radiographs, among others. These methods are in most cases time-consuming and costly, thus requiring structures to be located in accessible locations and heavily dependent on the skill and experience of the professional performing the inspection [10, 11].

In view of this scenario, there is a need for more viable structural monitoring methods. In view of this, structural

✉ Guilherme Ferreira Gomes
guilhermefergom@unifei.edu.br

1 Mechanical Engineering Institute, Federal University of Itajubá, Itajubá, Brazil

2 Institute of Industrial Engineering and Management, Federal University of Itajubá, Itajubá, Brazil

health monitoring (SHM) technology emerges as a promising alternative, by continuously monitoring the structure through the use of integrated sensors. This method brings with it great security because it detects failures and prevents them from evolving at an alarming level [12].

The objective of the SHM methodology is to provide the necessary tools for the structural monitoring in a constant or periodic way, in order to determine the need for corrective actions and to prevent catastrophic failures. Therefore, the application of this methodology has great potential in many areas of engineering, especially in the aerospace, civil and mechanical areas. The purpose of the SHM system is to allow the structure to be analyzed and monitored autonomously [13].

A large amount of research on the SHM methodology has been developed around the world due to the benefits and advantages that this methodology encompasses [14–20]. The work developed here consists of the use of the SHM methodology in structures of composite material, for which all necessary conceptualization will be presented in the next sections.

Equally important, it is known that the performance and behavior of mechanical structures made by CFRP can be significantly affected by degradation [21, 22]. This degradation could be caused by exposure to environmental conditions or damage caused by handling conditions, such as impact and overloading. Such damages are not always visible and obvious on the surface and could potentially lead to catastrophic structural failures.

Non-destructive inspection/evaluation (NDI/E) techniques such as of X-rays, ultrasonic waves, eddy currents, shearography, and infrared thermography are often employed for the detection, localization, and quantification of flaws and damage in composite materials [23]. However, these methods depend on the skill and experience of an operator. The creation of an effective and autonomous method, approached in this study, enables the SHM methodology and thus avoids the identification of false positives or negatives.

In like manner, NDI/E improves safety and often minimizes premature replacements and inspections can represent significant down-time. The aerospace industry has the most noteworthy result for SHM since damage can lead to disastrous (and costly) failures, and the vehicles involved have regular costly inspections. Currently 27% of an average aircraft's life cycle cost is spent on inspection and repair, so it becomes necessary to develop in situ monitoring methods [24].

Furthermore, according to [24], damage detection in CFRP is much more difficult due to the anisotropy characteristics of the material, the conductivity of the fibers and the fact that much of the damage often occurs beneath the top surface of the composite laminate, for instance with barely visible impact damage (BVID).

Often, according to [25], damage develops over a certain period of time (months or years), and is not immediately visible to even the trained operator's eye. However, once the size of the defect or stress-raiser reaches a critical value, failure can be catastrophic and the consequences severe. Plainly, there is a solid need to recognize as well as characterize the various types of damage and defects that occur in composite materials during technical operations. Unfortunately, there is no coherent overall design philosophy for accommodating such defects and damage in composite parts. Apart from the use of the design allowable strain limit, the approach has been generally of an ad hoc nature [25].

In essence, SHM of composite components is vital to the use in composite applications. Being highly susceptible to impact damage, those materials can sustain internal damage that is very difficult to detect externally. Thus, a SHM system could remove the uncertainties that are present in the design and implementation of composites in an aerospace application leading to optimized structures [26, 27].

A justification for using digital image correlation (DIC) is due to a non-contact optical technique to measure contour, deformation, vibration and strain on almost any material. The technique can be used with mechanical tests including tensile, torsion, bending and combined loading for both static and dynamic applications. The use of the digital image correlation technique is justified by the possibility of identify damages in composites, from the initial (matrix microcraks) to the final phase (fiber failure). DIC can reveal the elementary mechanisms in composites such as microcracks, debonding and delamination [28]. It was shown that damage laws can be identified with the help of DIC from mechanical tests imaged at different stages of loading. The complex damage type and failure mechanics theory present during the loading stage in a CFRP laminate are increased due to the presence of a stress concentration factors, causing a wide range of effects, such as stress or strain gradients fields [29]. It is therefore more desirable when performing experimental testing on laminated composites structures to obtain extensive full-field strain data, rather than limited strain (by a limited number of sensors) or displacement measurements obtained from traditional electrical strain gauges or extensometers.

This paper aims the damage identification by using an inverse problem method. The inverse problem is solved by the minimization of an objective function composed by mechanical strains (strain field) in CFRP structures (beams and plates). As it is an identification problem, metaheuristic algorithms are recommended [3, 30–32] because they have the capacity to deal with complex multimodal functions. Several algorithms of this class are developed in order to efficiently handle this task [33–36]. Optimization algorithms such as GA, PSO, and ACO were used to solve inverse damage identification problems. Recently, a new

SFO [37] metaheuristic was developed especially to address this type of problem and presented superior performance for the global identification of damages.

When trying to identify damage from a mechanical testing, the first step deals with the measurement of those displacement/strain fields. DIC showed an advantage over other methods [28]. As well stated in [28], the problem consists of the evaluation of the local elastic properties, expressed as a relative loss of stiffness (damage).

There have been various investigations in the literature using full-field measurements to examine the mechanical response of damaged composite structures under mechanical loading. Be that as it may, just a predetermined number of studies focuses on the assessment of the damage process in damaged CFRP structures using digital image correlation techniques has been applied before. When compared with the special requirement of traditional measurement techniques, DIC is a functional method because it takes advantage of the natural speckle pattern on the specimen and only needs a common camera and a computer to store the images to be subsequently analyzed [38].

All these observation suggest the advantage of the use of DIC in SHM system in order to identify damages in early stages which could be catastrophic especially for composite structures and which might not be captured by the traditional off-line testing techniques such as C-scanning and X-ray radiographs. The main objective of this work is the identification of structural damage through the numerical-experimental application of the sunflower optimization (SFO) algorithm coupled with the finite element method (FEM) and digital image correlation (DIC).

A deep numerical study of damage identification in laminated composites structures is made as in inverse problem methodology in this present study. The results show a substantial precision in terms of predicting the correct damage position. Although many studies have been reported on structural health monitoring in composites, very few have been focused on the use of the finite element method and optimization algorithms, especially by the use of the digital image correlation. The work presented here assesses the potential of this technique as the main tools in the inverse problem solution.

To the authors' best knowledge, there are no (or very scarce) studies in the literature investigating the use of DIC and optimization in damage identification problems, especially about the SFO. This paper is the first to do so. In other words, this paper investigates the use of SFO with online structural strains in order to identify the damage location. Experimental results showed the excellent efficiency of DIC and SFO in accurately detecting damage.

This manuscript is organized as follows: Sect. 2 a general bibliographic review is presented, addressing the scientific innovation about the subject and the main methodologies applied in this paper. Section 3 methodological procedure (direct and inverse formulation) is presented. Section 4 presents the main results and discussion about the damage identification. Finally, Sect. 5 draws the conclusions.

2 Background

2.1 Structural health monitoring in composite structures

Structural health monitoring (SHM) is an engineering area that works with innovative methods of structural monitoring; in general, monitoring takes place without affecting the integrity or performance of the structure. This technology integrates a group of factors that are used together, usually using nondestructive evaluation (NDE) coupled with sensing techniques and special materials to create greater reliability and to give a longer material life [32, 39];.

Structural damage may have different meanings in SHM, and it may be an imperfection, a defect, or a failure, which can be found when compared to a model under proper working conditions. A model in an adequate working condition is modeled with a data input that contains the physical characteristics of the structure and also the boundary conditions of that structure, that is, under which conditions of stress and packing this structure is submitted. The data output should give a correct or very close measurement of the damage to be detected by SHM [40, 41].

Different methods of damage identification are being developed, but all methods are classified based on models to be detected through captured signals. Vibration-based methods, for example, use physical and modal parameters to detect damage. The use of the model is fundamental so that the correct monitoring can be done, in order to obtain with truthfulness the information regarding the analyzed structure [42, 43].

Most methods that use signal processing are based on the relationship between the structural condition and the symptom given by the collected signal. According to [44], this relationship of the evidence given by the signal is not simple and its analysis is quite complex in structures used in engineering and furthermore requires the use of advanced materials.

According to [45], the detection of damage is a pattern recognition problem. Pattern recognition requires the selection of procedures usually based on statistics and approach to neural networks. The recognition of standards becomes essential for the implementation of an SHM system.

For [46], the structure examination is divided into 5 levels. The first one detects the existence of damage in the structure, the second locates the position and the dimension of the damage in the structure, the third level does an evaluation of the damage in the structure, the fourth realizes a forecast of the life of the structure, and finally the fifth level does a prognosis of structure damage.

The study developed here works exactly in the first two levels, i.e., detection and identification of the damage location in which the presence of a damage in the structure is first detected and subsequently there is an effort to locate the position and dimension of the damage.

SHM is a very broad and interdisciplinary field of research. It is dependent on several areas of studies such as materials science, mechanical systems, electronic systems and advanced computational techniques. Figure 1 shows schematically the interdisciplinary of the SHM system.

In summary, SHM is dependent on several distinct engineering sectors that work together to carry out structural monitoring. For [44], the sectors are: signal processing, sensors and actuators, non-destructive testing, computer (hardware and software) and knowledge of the structure to be monitored.

2.1.1 Monitoring in composite materials

Composites materials have some special characteristics such as good mechanical and thermal properties, longer life, rigidity, resistance to abrasion and corrosion, and it also has low specific mass. These characteristics make the composites widely used in industry in general and especially in the aerospace industry. A composite material is a material made of two or more distinct phases with different physical or chemical properties separated by an interface. When phases are well combined, this produces a material with better characteristics from the individual components. One phase is the matrix, generally based on a homogeneous and monolithic material in which the reinforced phase is embedded. Reinforcements for composites can be fibers or particles [47–49].

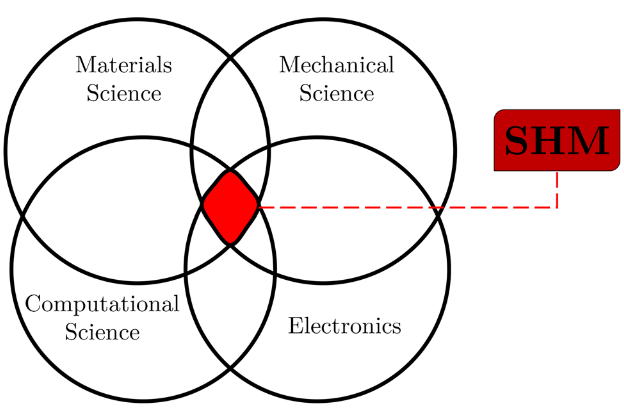

Fig. 1 The interdisciplinarity of an SHM system (Adapted from [44])

Health monitoring in composite materials becomes somewhat more complex than in metallic materials where damages are easily detected and in some cases perceptible human vision. In the case of composite materials, most of the time an erroneous perception occurs since the structure presents excellent surface conditions while inside the material serious damages have occurred [50].

The main problem of the use of composites in structures is the occurrence of delamination. It occurs when the structure is subjected to impacts at low velocity or when repetitive cycles of stresses occur, with this may occur a separation between two overlapping layers, this phenomenon is called delamination [51, 52].

For [53], structures composed of composite materials present a very wide variation of damages and a very variable behavior and with this they become very difficult to predict and to classify.

Many studies [54–56] and [3] showed that vibration methods are reliable to monitor composite structures. The composite material exhibits faults such as cracks in the matrix and fiber breakage, but these damages caused in a composite material produce similar changes in the vibration response caused by a damage in metallic material.

2.1.2 Stress concentration factor in composite plates

Analyzing and understanding stress and strain concepts will be important in this work because the damage criterion will be given by comparing and recognizing strain and stress patterns in numerical and experimental tests [57, 58].

The stress can be defined as the intensity of internal forces acting between the particles of a cross section of a body of deformable material. These internal forces can be defined as forces of reaction to external forces applied in the body to be studied. A body can be subjected to different types of external forces, but they will always be classified as field force or surface force. In all tests carried out in this work, the forces exerted on the structure are surface forces since there is direct contact between the structure and the test machine [59, 60].

The strain of a body can be defined as any change in the geometric configuration of the body that leads to a change in its shape or dimensions after the application of external forces. The strains can be easily visible or practically imperceptible if equipment that measures with high precision is not used [61].

When the internal force lines tend to become denser in a particular region of the structure, there is a strong indication that stress concentration may be occurring in this region. As the strength of a material is maximal when the forces exerted on it are distributed in the most uniform way possible, when the stress concentration occurs it can be said that this material loses resistance, since the distribution of forces in the material are not uniform [62].

In composite materials, most of the failures caused by stress concentration come from regions where there is discontinuity in the material, like porosity and delamination [63]. The concentration of stress in composites is dependent on the degree of anisotropy and the homogeneity of the material, the degree of anisotropy increases the stress concentration in the structure [64].

Tan [65] showed that the stress concentration in composites can be defined as the stress concentration factor (SCF) in which the stress increase is proportional to the increase in the stress concentration factor. In sequence, the SCF is dependent on the strain magnification factor (SMF). The use of SCF through SMF allows a direct comparison between numerically found values and values found experimentally. Finally, this study also shows that the change in the SCF factor changes the mechanical properties of the material. In this study, [65] also shows the values of the relationship between SCF and SMF factors [62].

The stress concentration factor for an orthotropic panel subject to uniaxial stress with an elliptical hole (Fig. 2) is calculated in [65]. A viable approximate expression valid for the range $0 \le b/a \le 1$ is shown in Eq. 1.

$$\frac{K_{t\infty}}{K_{tg}} = \frac{\lambda^2}{(1-\lambda)^2}\sqrt{1+(\lambda^2-1\left(\frac{2a}{H}\right)^2} - \frac{\lambda^2(2a/H)^2}{(1-\lambda)\sqrt{(\lambda^2-1)(2a/H)^2}} + \frac{\lambda^7}{2}\left(\frac{2a}{H}\right)^6\left(K_{t\infty}-1-\frac{2}{\lambda}\right)\left\{\left[1+(\lambda^2-1)\left(\frac{2a}{H}\right)^2\right]^{-5/2} - \left(\frac{2a}{H}\right)^2\left[1+(\lambda^2-1)\left(\frac{2a}{H}\right)^2\right]^{-7/2}\right\} \tag{1}$$

where $\lambda = b/a$ and $K_{t\infty}$ is the stress concentration factor for a panel of infinite width. For a laminate plate, the stress factor can be calculated as shown in Eq. 2. K_{tg} denotes the gross concentration factor.

$$K_{t\infty} = 1 + \frac{1}{\lambda}\sqrt{\frac{2}{A_{66}}\sqrt{A_{11}A_{22}} - A_{12} + \frac{A_{11}A_{22}-A_{12}^2}{2A_{66}}} \tag{2}$$

where A_{ij} denotes the effective laminate in-plane stiffnesses with 1 and 2 parallel and perpendicular to the loading directions, respectively.

In terms of the familiar material constants, the stress factor can be expressed as shown in Eq. 3.

$$K_{t\infty} = 1 + \frac{1}{\lambda}\sqrt{2\left(\sqrt{\frac{E_x}{E_y}} - \nu_{xy} + \frac{E_x}{2G_{xy}}\right)} \tag{3}$$

where E_x and E_y are Young's moduli in the x and y directions and G_{xy} and ν_{xy} are the shear modulus and Poisson's ratio in the x, y plane.

The approximate K_{tn} can be obtained from the relationship between the net and gross concentration factor as shown in Eq. 4.

$$K_{tn} = K_{tg}\left(1-\frac{2a}{H}\right) \tag{4}$$

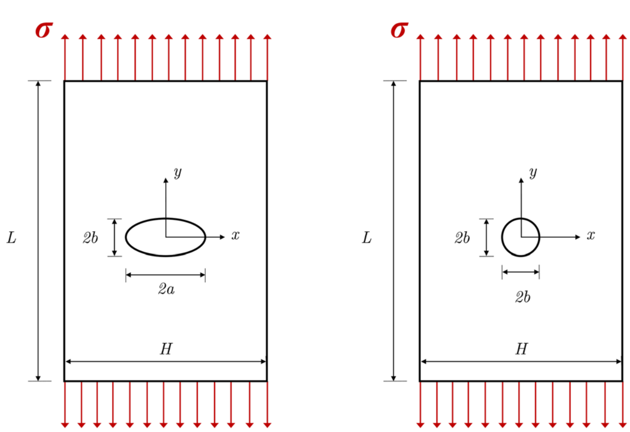

Fig. 2 Finite-width panel subjected to stress with a central elliptical hole (adapted from [62])

For a circular hole ($\lambda = b/a = 1$), Eq. 1 can be rewritten as Eq. 5.

$$\frac{K_{t\infty}}{K_{tg}} = \frac{2-(2a/H)^2-(2a/H)^4}{2} + \frac{(2a/H)^6(K_{t\infty}-3)[1-(2a/H)^2]}{2} \tag{5}$$

with $2a = d = r/2$, where d and r are the diameter and radius of the hole, respectively.

2.2 Digital image correlation

Digital image correlation (DIC) is an optical technique that consists of analyzing the surface of a structure before and after undergoing a load to determine fields of displacements and strains. It is also used to determine stresses and thus has a wide field of application in science and engineering [66].

When comparing DIC with conventional methods such as strain gauges or Strain Gages, DIC provides a greater wealth of information during the trials, since it can analyze a much wider area than that analyzed by conventional methods [67, 68].

Peters and Ranson [69] was one of the pioneering works carried out in the area of digital image correlation. The authors showed techniques to experimentally perform a stress analysis on the structure. Equally important, [70] developed an algorithm using image correlation for the measurement of displacement in the plane. Shortly thereafter the DIC technique was already being studied by several researchers. Most of the works currently test new applications and equipment. The search for improvement in algorithms for computational speed gain and consequently for better efficiency is one of the largest research niches in this area [70, 71]. However, none of them addresses an inverse problem of damage identification, as proposed in this study.

The data processing programs of the DIC technique relate the light intensity of various regions composing the image containing the complete surface of the structure tested. The data-processing program determines the mean of the subarea displacements analyzed in the initial and final images of the trial. The determination of displacement occurs when a sub-region of the undeformed image is identified in the deformed image. This identification is achieved through algorithms that seek the correlation between the light intensities contained in the sub-areas of the image before and after the effort occurs [72].

The use of the DIC technique in composite materials has very satisfactory results, it is generally used to aid in the detection of defects in these materials and, as a consequence, it helps in the studies about the causes of these failures. The efficiency of DIC is related to the wide range of strain rates in which it operates [73, 74].

In two-dimensional digital image correlation, displacements are directly detected from digital images of the surface of an object (specimen). Figure 3 shows a typical example of an experimental setup for two-dimensional digital image correlation. The plane surface of an object is observed usually by a CCD (charge-coupled device) camera with an imaging lens. Then, the images on the surface of the object, one before and another after strain, are recorded, digitized and stored in a computer as digital images. These images are compared to detect displacements by searching a matched point from one image to another [75].

2.3 Sunflower optimization (SFO)

Optimization can be defined as a process of searching for the best solution within a set of possible solutions. The optimization methods can be divided into two large groups, being mainly divided into local and global optimization methods. The first method is based on calculations, whereas the second method is based on heuristics. Briefly, what differentiates them is that the local optimization methods develop their searches from a single point, that is, a single solution, whereas the global optimization methods generate a population of initial points and these points are possible solutions, and points represent the best solution to the problem [76].

Many optimization techniques have been developed with inspiration in nature. The particle swarm optimization (PSO) [77], ant colony optimization (ACO) [78] and differential evolution (DE) [79] are examples of these techniques. These techniques are able to solve difficult problems found in mathematics and engineering; however, there is no way to highlight a single method as the best to solve all kinds of problems, since each algorithm has strengths and weaknesses [80].

It is in this scenario that the sunflower optimization algorithm (or simply SFO), which is based on the flower pollination algorithm proposed by Yang [81] becomes extremely important because it is highly capable of solving a problem of multimodal optimization with non-explicit functions. The SFO is based on the analysis of the behavior of sunflowers

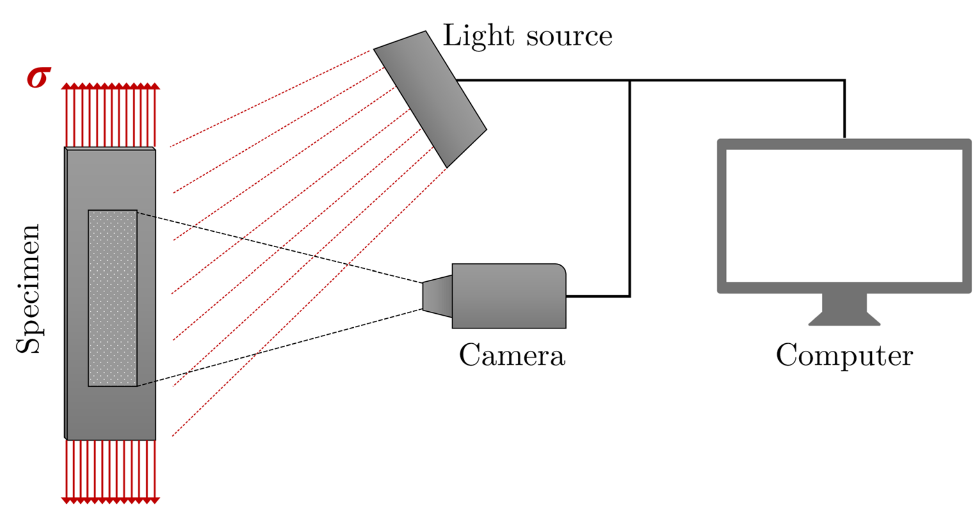

Fig. 3 The main setup for displacement measurement using digital image correlation (Adapted from [75])

that are always in search of the best orientation to the sun. Each day these plants perform a cycle, in which they accompany the movement of the sun, always orienting towards the same, and during the night they return to the initial position and continue the ritual the next day. The operation of the SFO algorithm can be understood by the following description, developed and presented in [37].

The algorithm starts by generating an initial population of individuals (flowers), and can be generated in a random or ordered way according to the requirements of the problem. The algorithm then calculates the fitness of each individual in this search space, quantifying this value as fitness function. The best individual(s) of this flower population will be defined as the reference of the search space, that is, the sun. In the same way that sunflowers are oriented by the sun in the world we live in, all individuals will be guided by the plant with the best suitability in the population in this method of optimization. Once guided by the sun, individuals will reproduce and move toward the optimum point in a controlled random fashion, i.e., new individuals will be generated randomly, however, in a particular specific direction.

This algorithm works with three main variables defining the biological operators, being: (i) pollination rate (p_p), (ii) plant mortality rate (m_p) and (iii) the survival rate of plants that will move in a controlled manner until the sun (p_s).

The pollination rate p_p defines the percentage of individuals in the population who will pollinate with each other. It is also worth noting that the pollination considered is randomly taken along the minimum distance between flower i and flower $i + 1$, that is, the best individuals will pollinate hierarchically with each other. In the real world, each flower usually releases millions of gametes of pollen. However, for simplicity, it is also assumed that each sunflower produces only one pollen gamete and reproduces individually.

The mortality rate m_p determines that a percentage of individuals will not survive because they are too far from the sun and did not receive enough heat for their survival. m_p% individuals will be defined as the worst in their population according to the value of their respective skills. This biological operator is fundamental to the developed heuristic, since it allows a certain variability of the population throughout the generations and reduces the probability of obtaining regions of great places.

The third variable p_s characterizes the percentage of individuals that will move toward the heat source (sun). It is clear that in nature the plants (or the vast majority of them) do not have movements of translation. However, in this case, a movement is attributed to the especial percentage of the individuals of the population. The step size given by the surviving individual will be random according to a normal distribution, between their location and the location of the best individual (sun). The survival rate is then defined as $p_s = 1 - (p_p + m_p)$, because $p_p + p_s + m_p = 1$.

The problem addressed in this study is an identification problem, where the parameters to be identified correspond to the location and dimension of a structural damage. To solve an inverse/identification problem, several optimization algorithms can be employed. However, as it is a complex functional, multimodal and with an implicit objective function (only output values when outputting the numerical response through FEA) metaheuristic algorithms are recommended [3].

Several metaheuristic algorithms have been developed and applied to damage identification problems, such as genetic algorithm (GA), particle swarm optimization (PSO), bat algorithm (BA), firefly algorithm (FA), ant colony optimization (ACO) and many others. In this study, we opted to use the SFO algorithm because it is a new metaheuristic that was developed especially to address structural damage identification problems [37] and presented results superior to another metaheuristics for this specific application. This fact justifies the choice of this metaheuristic in this work. The advantage of the SFO algorithm over other metaheuristics (for this specific application) can be explained by its non-complexity of several control parameters and a combination of exploration-exploitation that allows a high capacity for global search and local refinement.

3 Inverse problem methodology

3.1 Direct problem: finite element modeling of composite laminated plate

The finite element method (FEM) is usually adopted to solve direct problems in structures, that is, for a given load (input), one can determine the strains that the structures undergo (output). In this way, the method can be applied, for example, to verify and validate a project, to obtain improved predictions of structural response, or simply to identify unknown characteristics of the system [37].

Both structures are of the same material with different geometric properties. In general, we considered the case of a specimen subjected to a uniaxial tensile stress at one of its ends, subject to a clamped condition in its end (Fig. 4). The geometry in question is a beam and plate in which the damage is contained in the $x - y$ plane. This type of shell geometry was motivated by being able to resemble most cases and problems in aerospace structures.

It is known that this configuration promotes a particular voltage stay and that the presence of a geometric damage promotes a change in this initial configuration. Therefore, it was evaluated the state of strain of the test cups and for this, we considered the information coming from a finite number of sensors, i.e., 8 sensors (s_1,s_2,...,s_8). The sensors were distributed symmetrically in the structure as shown

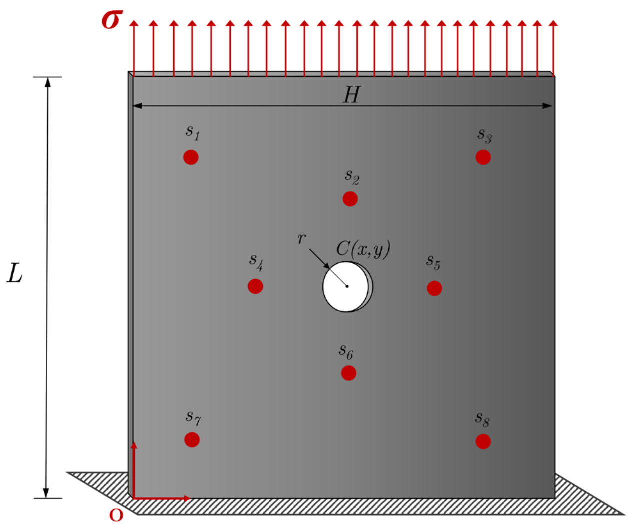

Fig. 4 The direct problem: clamped composite laminated plate under axial loading. Damage is modeled according to three design variables

in Fig. 4. The information from these sensors was used in the formulation of the inverse problem detailed in the following section.

As for the model used in this work, two structures were considered: i) beam and ii) plate, one of the plate type and the other of the beam type, both with small and uniform thickness. The plate and the beam in question were modeled using shell elements with eight nodes and six degrees of freedom per node (translation and rotation with respect to the x, y and z axes). The mesh quality is essential for obtaining good results, so we chose to use a structured, two-dimensional mesh throughout the entire structure, including the hole region, as can be seen in Fig. 6.

Regarding geometry, the two shaped structures were a square plate with sides $L = H = 30$ cm and a rectangular beam with $L = 30$cm and $H = 3$cm. Both structures consist of a symmetrical laminate of composite material consisting of 12 layers of different orientations arranged in the form $[0/90]_{3S}$; both layers have thickness's equal to t=0.1824 mm. The set of main properties of the material used in problem modeling is presented in Table 3. After all the modeling of the structures, the application of a uniformly distributed load on the ends of the structures was modeled, in order to generate tensile forces in both.

It is known that a structural damage can be modeled by means of a modification of the physical or geometric properties. In this context, the damage was approached as a geometric modification of the studied plaque. The damage was imposed by means of circular holes in two different situations: *i)* for the beam model, a hole with radius $r = 6$ mm was used and for *ii)* a hole plate with radius $r = 10$mm. Both damages correspond to less than 1% of the total area of the initial structure.

Table 1 Mesh size convergence for maximum, minimum and average strains on the y axis

Mesh size (mm)	ϵ_{min} $(\mu\epsilon)$	$\overline{\epsilon}$ $(\mu\epsilon)$	ϵ_{max} $(\mu\epsilon)$
1.00	62.72	123.85	155.26
2.00	62.54	123.61	154.95
4.00	62.53	123.60	154.93
8.00	62.53	123.59	154.93
16.00	62.53	123.59	154.93

Before discretizing the model in finite elements, and even before building it, it is important to think about the mesh concept. Thus, shell elements were generated, mapped over the structural surface with eight nodes and six degrees of freedom per node. Table 1 shows the results obtained in the mesh convergence study. In addition, Table 1 shows the values of the maximum, average and minimum deformations along the longitudinal axis y. The choice of discretizing the structure with elements of 2 mm in size is justified because it saves computational effort, since this modeling leads to obtaining information without loss of quality when compared to a more refined modeling. In addition, Fig. 5 shows the graphical results for the strain response considering different mesh sizes.

An analysis of the finite element model's discretization errors is estimated using Richardson's extrapolation method [82]. In this method, the estimated error of the numerical solution due to a coarse mesh size h_1 is defined by Eq. 6 [83].

$$e = \frac{y_2 - y_1}{1 - r^p} \tag{6}$$

where $r = h_2/h_1 = h_3/h_2$ is the mesh refinement rate, y_1 and y_2 are the responses obtained using a coarse and refined mesh, respectively.

The p convergence order can be estimated by Eq. 7.

$$p = \frac{\ln\left(\frac{y_3-y_2}{y_2-y_1}\right)}{\ln(r)} \tag{7}$$

where y_3 is the response related to the smallest mesh size.

Table 2 displays the results of the numerical analysis (FEA) considering different mesh sizes with a refinement rate $h = 0.5$ applied twice in the discretization of the 4-mm mesh ($h_1 = 4$), obtaining y_1 for values of $h_1 = 4$, y_2 for $h_2 = 4$ and y_3 corresponding to $h_3 = 1$. From the values of *epsilon* in Table 2, one can assume what the value would be considering an extremely refined mesh.

After the due calculations obtained by Eq. 6, the largest error calculated for the strain is obtained (Table 2) has a value of 13.26 for the minimum strain. However, in the formulation of the objective function used in the methodology of this work, only the maximum deformations were

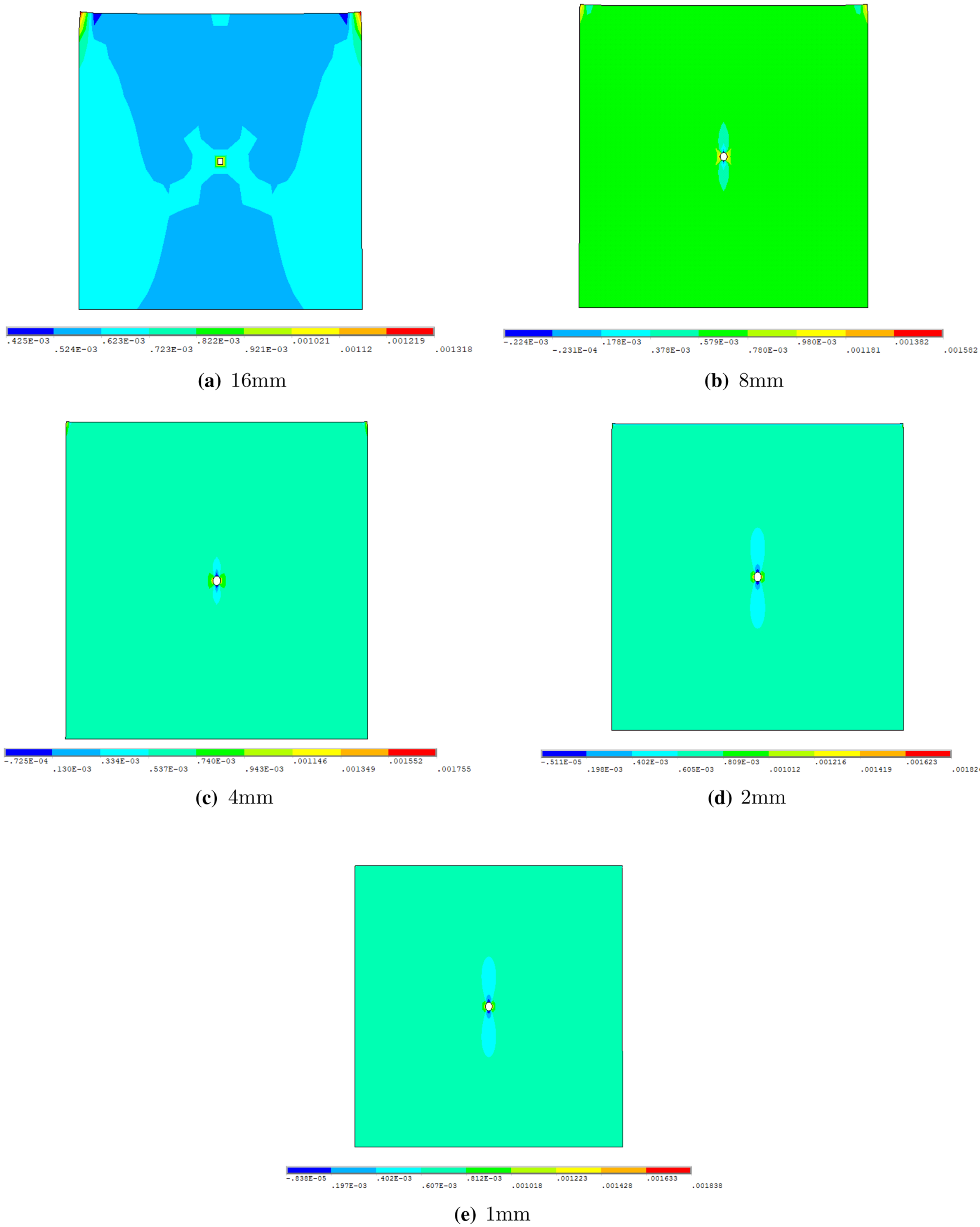

Fig. 5 Strain response for different mesh sizes

Table 2 Quantification of model discretization errors

Response	y_1	y_2	y_3	p	e	Y	Error (%)
ϵ_{min}	60.10	53.80	51.10	1.2224	−11.0250	47.50	13.26
$\overline{\epsilon}$	624.97	625.53	625.84	0.8532	1.2544	626.09	0.09
ϵ_{max}	1755.00	1826.00	1838.00	2.5648	88.4407	1897.00	3.74

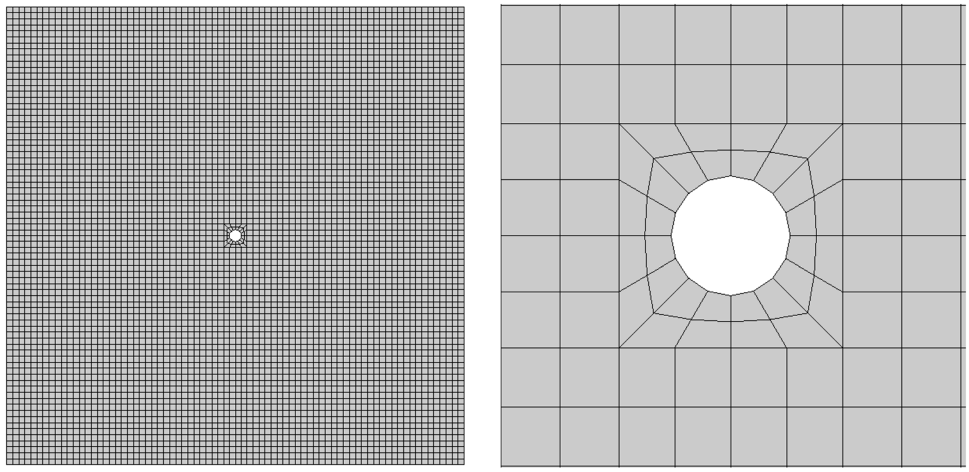

(a) Meshed plate with circular hole **(b)** Zoomed region with hole

Fig. 6 Detail of the mesh in the region of the hole

Table 3 CFRP material properties used in the numerical modeling

Property	Value
E_1	88.8 GPa
$E_2 = E_3$	6.3 GPa
$G_{12} = G_{13}$	8.3696 GPa
G_{23}	2.3849 GPa
$\nu_{12} = \nu_{13}$	0.3208

used. Therefore, it is concluded that the model discretization error is not relevant (3.74 %). Therefore, the structure discretized in with 2-mm elements is adequate.

It was decided to use a mapped mesh for the discretization of the structure with the circular hole [84, 85]. Further care was taken so that the mesh containing the hole was sufficiently refined in the vicinity of the bore so as to sensitively capture the stress concentration arising from this geometric discontinuity. It was then decided to maintain the refined mesh throughout the entire structure according to the pattern near the hole. A coarser mesh outside the hole region could be maintained without loss of quality in the results, which would save computational cost.

The quality of mesh is an important aspect for stress concentration related problems. This is because the accuracy of solution depends on the mesh density around the stress concentrator. For reasonable solution, the mesh should be more refined near the stress concentrators to capture the local effects [84].

At the end of the modeling, Scilab® software was used to perform the complete inverse optimization problem using SFO. To obtain reliable results, 8 nodes located in different places of the structure were chosen.

3.2 Heuristic optimization programming

It is known that when a given structure has a damage, its structural properties are modified, thus becoming different from the properties of the initial structure (without damage). The inverse method has as objective to find the answer of the proposed problem to the optimization algorithm; that is, analyzing the properties of a structure, it is desired that the optimizer is able to solve the problem, determining the possible parameters of the damage.

In order to solve the problem of identification, an objective function is used and it is introduced in the algorithm and becomes able to provide the solution of the problem when it is properly minimized. The following is the objective function used in this work is built in function the strain differences about the pristine and damaged structure. The function in question is represented by Eq. 8, it can be observed that in this case the minimization is due to the difference between the known values of the strain of the actual damage and the calculated values of the strain of the damages obtained from the optimization algorithm. It is worth mentioning that all values of the strains were obtained by FEM.

$$J(\vec{X}) = \sqrt{\frac{1}{n}\left(1 - \frac{\epsilon_i^{\text{real}}}{\epsilon(\vec{X})_i^{\text{calculated}}}\right)^2} \quad (8)$$

where ϵ_i^{real} are the strain obtained from the real damaged structure, $\epsilon(\vec{X})_i^{\text{calculated}}$ are the strains obtained by SFO algorithm, $\vec{X}$ is the design vector that contains the damage variables, i.e., $\vec{X} = \{x, y, r\}$ and n is the number of strain points (or sensor points), in this case, n=10.

For the algorithm setup, the bounds were defined as shown in Eq. 9.

$$\{0.05L_x, 0.05L_y, 2\,\text{mm}\} \le \vec{X} = \{x, y, r\} \le \{0.95L_x, 0.95L_y, 12\,\text{mm}\} \quad (9)$$

where L_x and L_y are the dimensions of plate about the x and y axes, respectively.

As stated before, the algorithm employed here to solve the inverse optimization problem was the sunflower optimization (SFO). This algorithm was chosen for this type of problem because it is a new algorithm and has already presented better efficiency than the GA for damage identification in structures [37]. The algorithm proved to be efficient in dealing with implicit objective functions. An ideal combination of its three biological operators allowed great efficiency in the search for optimal global. Still, the phototropism characteristic of the sunflowers allows a better targeted random search.

3.3 Experimental testing using DIC

In an attempt to validate experimentally the optimization method employed in this work, an experiment was performed using the DIC technique. The experiment was carried out at the Laboratory of Destructive and Non-Destructive Testing (LEN) of Federal University of Itajubá (UNIFEI). A universal test machine of the brand INSTRON®, model 8801 with load capacity of 100kN was used to carry out the experiment.

In the experiment, the specimen was inserted to the universal test machine as shown in Fig. 7, after which it was subjected to a tensile stress (below the yield). During the experiment, it was decided not to submit the test specimen to compressive stresses due to the possibility of buckling

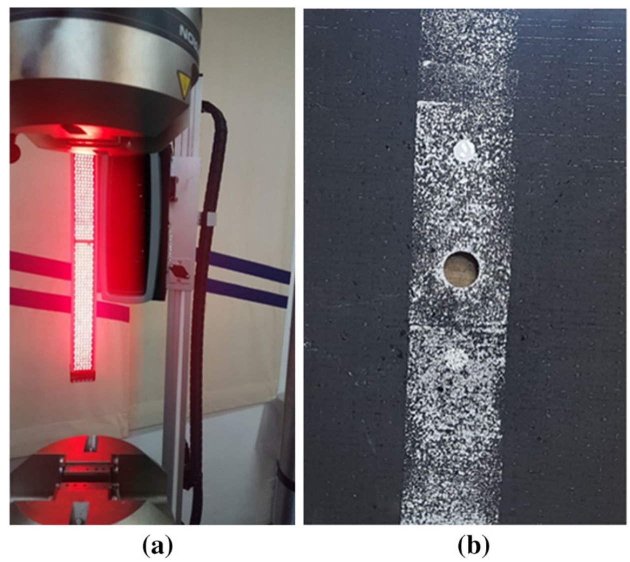

Fig. 8 Experiment details for the **a** data acquisition system and the **b** pattern of points on the specimen

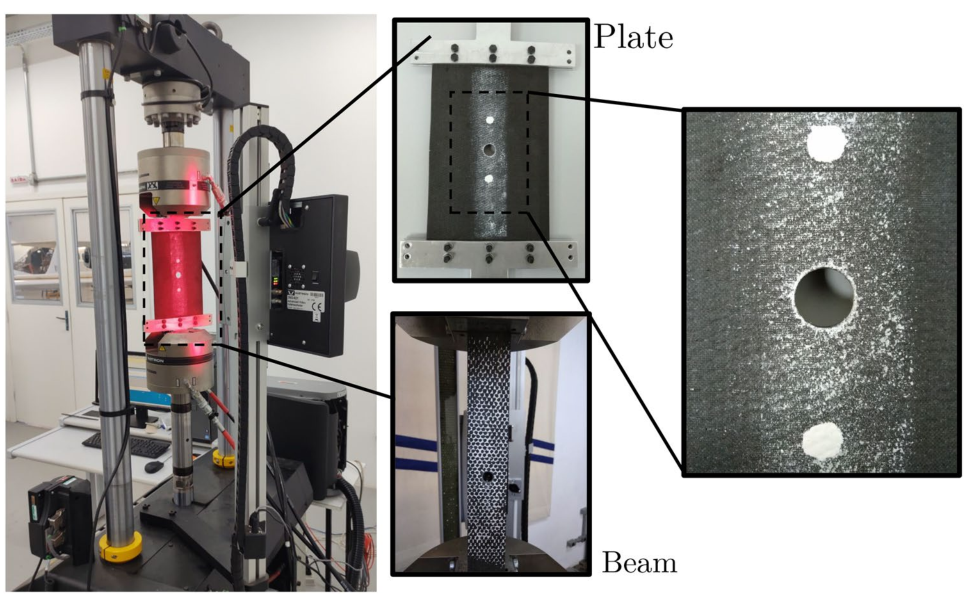

Fig. 7 Experimental setup performed for analysis on damaged beam and plate models

occurrence. Two cases were evaluated: (i) a plate and (ii) beam model in the presence of damages.

In order to capture the strains generated in the test specimen, a data acquisition system was used consisting of a camera with sensors and a computational apparatus, and this system can be observed in Fig. 8a. The resolution of the camera depends on the size of the measurement zone in question, while the maximum size of the measurement zone depends on the monochrome light emitter.

In order for the data acquisition system to work correctly, it is necessary that the background color of the test piece is dark, if it is not, the test piece must be painted. As the specimen used in the experiment was already black, there was no need to paint it. Next, paint the test specimen in a spray pattern using white paint. In this experiment, a sponge was used to make this painting; however, there are other methods that can be employed, such as the spray paint itself and even a toothbrush or brush. Figure 8b shows the specimen with this well-defined pattern.

After the experiment was carried out, all the data generated were collected and processed by Bluehill® software, which is also provided by INSTRON®, manufacturer of the universal testing machine and DIC data acquisition tools. The results obtained in this experiment are also presented and discussed in the next Section.

In Fig. 9, a flowchart is introduced to summarize all the methodology that was used in this work, from the initial problem to the solution of this problem, in it we can observe the existence of two slopes, one focused on the computational solution of the problem and the other solution to the problem.

4 Results and discussion

4.1 Numerical results

As already known, the work developed here aims to study the damage detection, which in this case is modeled as circular holes. This type of damage is said to be a complex damage in terms of numerical–mathematical modeling, since the vector of design variables has three variables (position x and y of the hole and its radius r). Thus, the purpose of this study is to verify the capacity of the SFO to detect these damages, through the analysis of strains.

Certainly, the choice of the meta-heuristic is fundamental. There is no algorithm capable of solving all optimization problems (no free lunch theorem). However, some play a better role for certain types of problems. The main objective of this study is to identify damage through the strain field obtained by DIC, which is a technique that does not have direct contact with the structure in question.

For the application of the algorithm, it is necessary first to define its variables, that is, its biological operators. These operators are the ones that coordinate the operation of the algorithm in the search for optimal regions [86]. The operators were chosen based on previous studies using SFO [37,

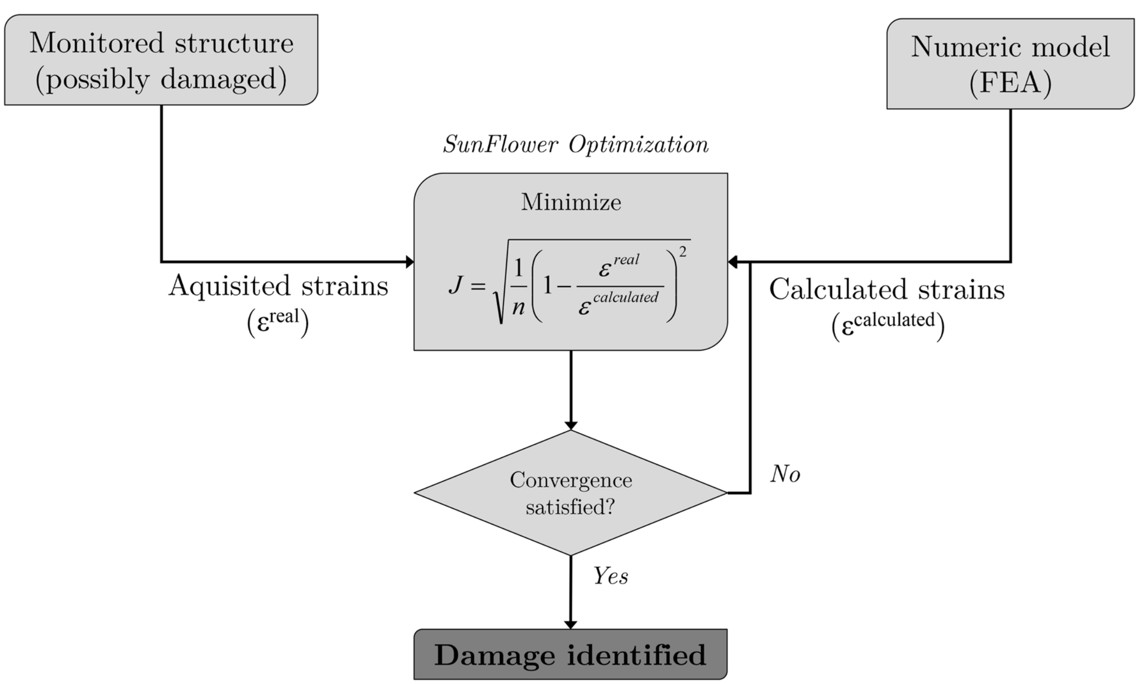

Fig. 9 Flowchart of the methodology used in this work

Table 4 Biological operators used in the sunflower algorithm

Operator	Beam	Plate
Flowers	70	100
Pollination rate	0.10	0.10
Mortality rate	0.10	0.10
Survivor rate	0.80	0.80
Number of suns	1	1
Generations (stop criteria)	70	50

87, 88]. The values of these control parameters are shown in Table 4.

A total of four distinct damage detection analyses were performed, two for the beam and two for the plate. Referring first to the beam, in the first analysis the damage (circular hole) was induced at the center of the beam, while in the second analysis the damage was induced at a random position of the beam; it is also noted that the hole radius is different in both analyses. The analyses performed on the plate occurred similarly to those performed on the beam. In all, 8 simulations were performed in each damage detection analysis. It is convenient to perform several simulations because the optimization technique employed in this work (SFO) is a heuristic technique, that is, it is based on random searches. Then, 8 simulations were established, completing a complete factorial (2^n). In this case, $n = 3$ with $\vec{X} = \{x, y, r\}$. Table 5 shows the results of all the simulations performed for the beam and the plate respectively.

As can be observed, the results presented in both tables were satisfactory, since all the parameters obtained converged to values very close to the actual damage parameters, and the damage was found (simulated) practically concentric and or tangential when compared to the actual damage. This can be easily seen in Figs. 10 and 11, which show the results of all cases presented in Table 5. Based on the results obtained, the robustness of the SFO is verified when applied in the detection of damage in both beams and plates.

Observing Fig. 12, it is possible to visualize the variation of the damage parameters (x, y and r) along the interactions (generations). It can be seen a greater variation in r than in x and y, with it being understood that the radius (r) was the most difficult parameter to identify, this can also be verified by analyzing the deviations in Table 5 in which the deviation of the radius (r) is considerably greater than the deviation of the positions (x and y).

The minimization of the objective function can be observed through Fig. 12d. By analyzing the behavior of the curve, there is a decrease in its value with the passing of the generations.

Because it is a zero-order algorithm, several simulations were necessary in order to obtain a mean. In some cases, the result was relatively further from the known damage. This can be explained by the fact that the objective function formulated, both mathematically and physically [3, 32]. In mathematical terms, a correct formulation can contribute to a better identification in terms of sensitivity. Due to the physical issue, the evaluated response may also be more susceptible to impairment as a function of the induced damage. In this case, it was chosen to formulate the objective function in terms of strains. It is known that a geometric damage generates a stress/strain concentration and this will generate sufficient perturbation so that the damage can be identified iteratively by means of the proposed method.

Regarding the computational cost, SFO proved to be more advantageous than other heuristics, justifying its use in this study [37]. In like manner, the proposed methodology evaluates each objective function 50×100, i.e., 5000

Table 5 Damage identification results considering the composite beam

	Beam structure						Plate structure					
	Damage I			Damage II			Damage III			Damage IV		
	x (m)	y (m)	r (mm)	x (m)	y (m)	r (mm)	x (m)	y (m)	r (mm)	x (m)	y (m)	r (mm)
Objective	0.0150	0.1500	4.0000	0.0200	0.1000	3.5000	0.1500	0.1500	6.0000	0.2100	0.1200	10.0000
Run 1	0.0150	0.1495	4.0012	0.0198	0.0996	3.7139	0.1503	0.1504	5.4779	0.2096	0.1199	10.4416
Run 2	0.0149	0.1545	4.0142	0.0199	0.0998	3.6454	0.1505	0.1509	6.2911	0.2110	0.1191	8.6687
Run 3	0.0150	0.1485	4.0015	0.0199	0.0999	3.5642	0.1507	0.1514	6.4873	0.2086	0.1282	10.5401
Run 4	0.0150	0.1501	4.0012	0.0201	0.1000	3.5446	0.1500	0.1499	6.0275	0.2098	0.1204	10.1733
Run 5	0.0150	0.1500	3.9985	0.0190	0.0995	3.5326	0.1496	0.1491	5.6982	0.2080	0.1388	9.7010
Run 6	0.0155	0.1498	4.0125	0.0198	0.0995	3.5245	0.1495	0.1490	5.0155	0.2090	0.1194	11.6074
Run 7	0.0150	0.1523	3.9987	0.0199	0.0990	3.5249	0.1510	0.1491	5.8051	0.2099	0.1195	10.2257
Run 8	0.0150	0.1542	3.9946	0.0200	0.0986	3.5513	0.1501	0.1503	6.0774	0.2095	0.1199	10.8712
Mean	0.0150	0.1511	4.0028	0.0198	0.0995	3.5752	0.1502	0.1500	5.8600	0.2094	0.1232	10.2786
Deviation	0.0002	0.0023	0.0069	0.0003	0.0005	0.0684	0.0005	0.0009	0.4695	0.0009	0.0070	0.8578

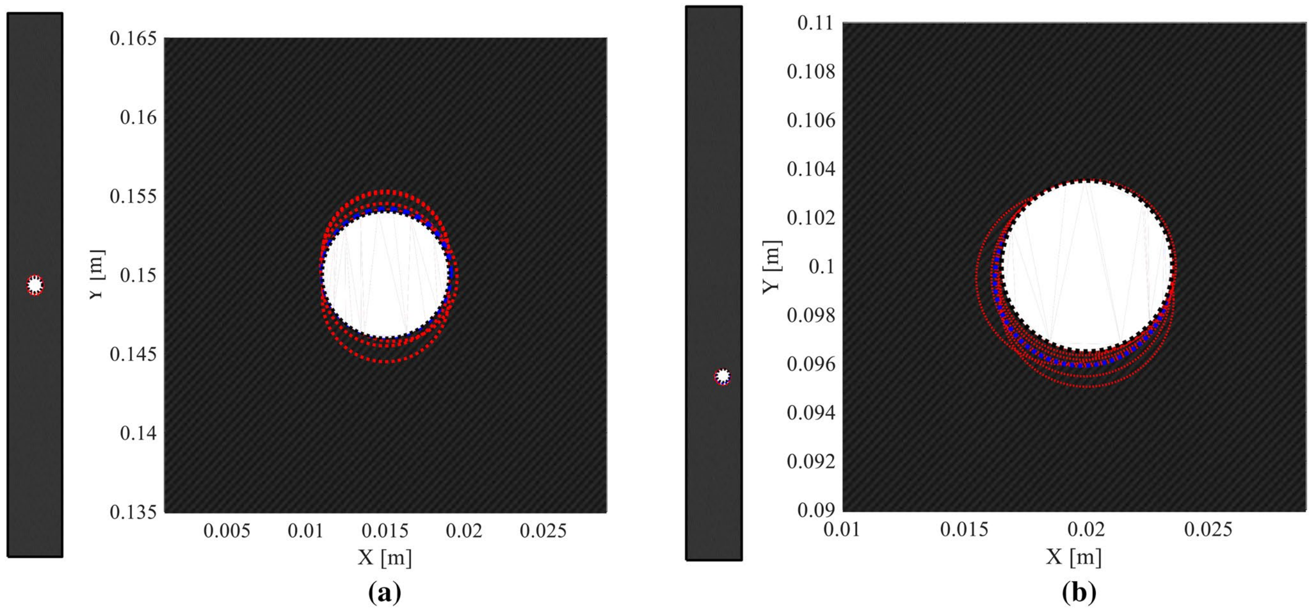

Fig. 10 Damage identification results considering the composite beam for **a** Damage case 1 and **b** Damage case 2 (legend: red dotted line; identified damages black dotted line; real damage blue dotted line; mean) (color figure online)

times (number of flowers x generations). For each evaluated objective function, a new solution is performed by FEM. Considering a simple personal computer (intel i5 processor, 6 Gb RAM), each function takes about 2 to 3 seconds to be evaluated in the FEM software interaction and Scilab®.

It is important to note that the results of this convergence started from the best individual in the initial population. The algorithm generated a random initial population within the bounds of the design variables (x,y,r). All individuals were evaluated, and then the one with the lowest objective function (fitness) was considered the best $x*$ (sun). In addition, different starting points were evaluated, since 8 runs were performed for each case, due to the stochastic characteristics of the algorithm. In other words, 8 initial populations for each case, which resulted in results very close to the ideal (induced damage).

4.2 Experimental results

In previous section, the FEM was used to model a test specimen subjected to a tensile stress, in this test body a hole was introduced whose parameters were known until then. From this, data regarding strains occurred at certain points of the specimen were extracted, and then, these data were used by the optimization algorithm in an attempt to detect the damage. As it was seen, the optimization method obtained satisfactory results, so that the holes identified were close enough to the actual holes (induced).

Now, in an attempt to validate experimentally the optimization method employed in this work, an experiment was performed using the DIC technique, in which a real test body was subjected to a tensile stress. From this, data were obtained regarding strains occurring in the specimen. And then it is these data that will be used by the optimization algorithm in an attempt to detect the damage present in the test body.

In the experiment, the beam (whose properties are already known) was subjected to a tensile strength of 19,620 N, suffering a maximum stress of approximately 300 MPa. The field of strain generated in the beam can be observed in Fig. 13a. By modeling through the FEM a beam equal to that used in the experiment and subjecting it to the same conditions of stress, the field of strain presented in Fig. 13b was obtained. Comparing the behavior of the two strain fields, we can see that both are quite similar. From Fig. 13, it can be seen that in the region of the holes there is a stress concentration, generating in this way, greater strains in this region, on the other hand, in the rest of the beam the strains are practically constant. Therefore, the strains generated in the beam can be a possible criterion to be used in the detection of damage.

The figure shows 13 results for axial deformation ϵ_{yy}. Figure 13a shows admissible strain results, while Fig. 13b shows the percentage of deformation. In a normalized character, both quantitatively have the same behavior, that is, stress/strain concentration around the damage. When considering the inverse optimization problem, a normalization becomes necessary. This standardization will be defined in the following paragraphs.

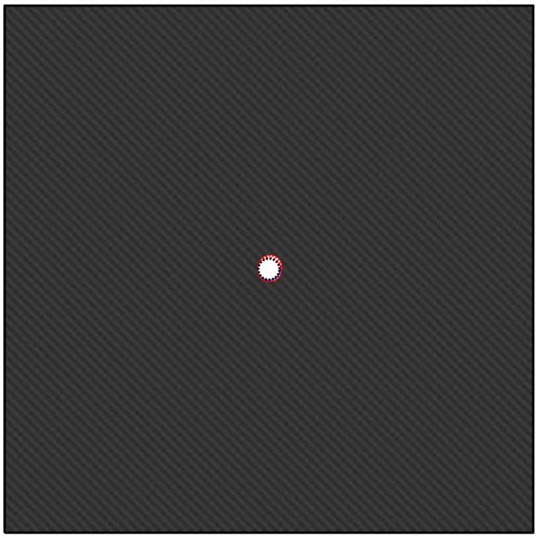

(a) Damage case III

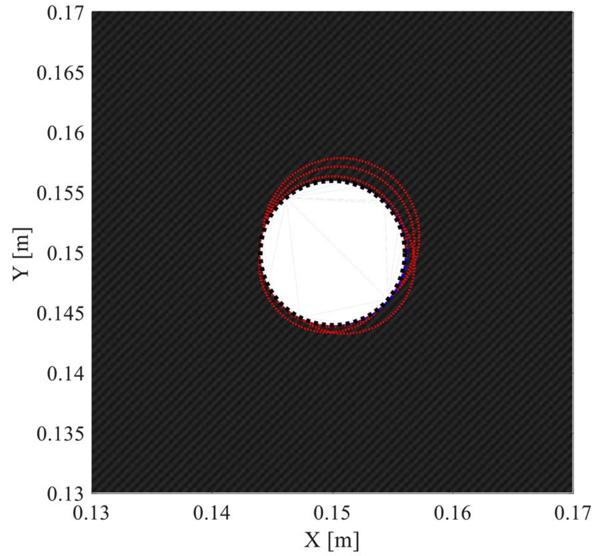

(b) Zoomed area for case III

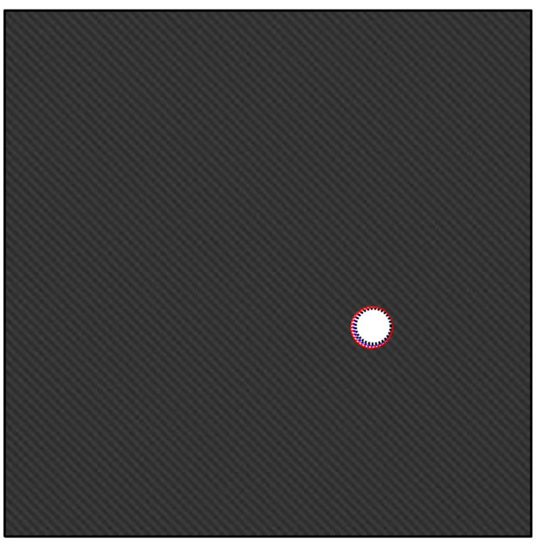

(c) Damage case IV

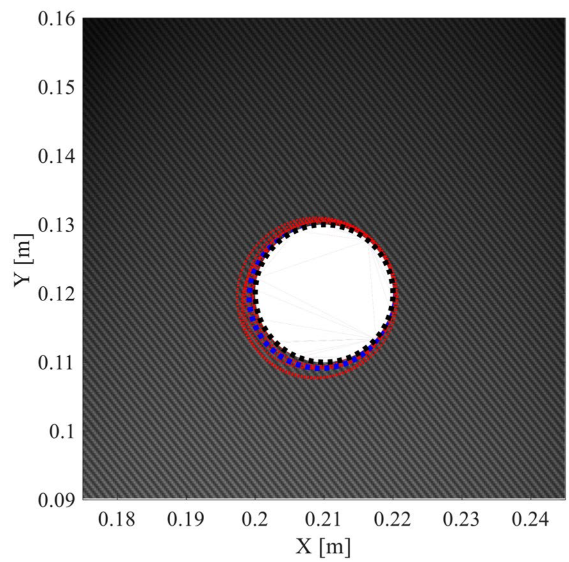

(d) Zoomed area for case VI

Fig. 11 Damage identification results considering the composite plate (legend: red dotted line; identified damages black dotted line; real damage blue dotted line; mean) (color figure online)

As the optimization algorithm uses the FEM in the process of identifying the damage, the results obtained through the DIC must be transmitted to the algorithm in the same unit of measurement used by the FEM. However, the strain units used in both methods are different, and in DIC the result is given in percentage unit (%) while in the FEM it is given in units of the international system, in this way, it was chosen to normalize the obtained results by the DIC to transform them into the same unit used by the FEM.

The data to be supplied to the optimization algorithm to identify the damage, must be in unit equal to the one used by the FEM. The strain data provided by the DIC are in percent units, hence the need to normalize these data, with the intention of transforming them into the unit used by the FEM later. The strain varies in a range from 0 to 2.25 (%); in this way, Eq. 10 can be applied to normalize the strain.

$$\epsilon_N = \frac{\epsilon}{\epsilon_{max} - \epsilon_{min}} = \frac{\epsilon}{2.25} \tag{10}$$

Now, with the normalized strain, it must be transformed to the strain unit used by the FEM; for this, we must carry out the inverse procedure to that performed above. The strains

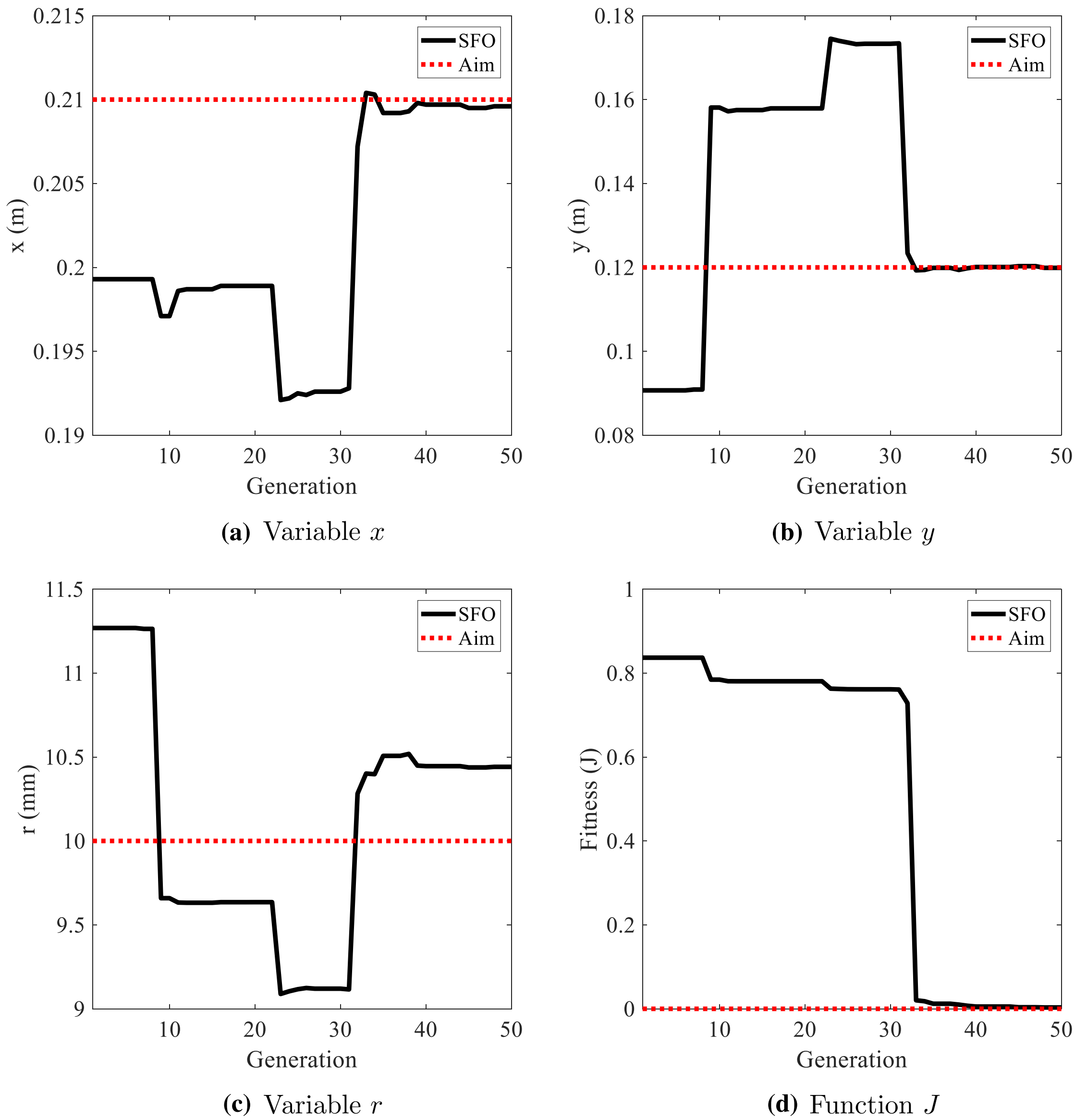

Fig. 12 Variation of parameters throughout a simulation

in the FEM vary in the range of 0.016921 to 0.412598; thus, if it were to normalize the strains, Eq. 11 should be used; however, as the normalized strain is already known and what is desired is the equivalent strain, it uses Eq. 12.

$$\epsilon_N = \frac{\epsilon - \epsilon_{min}}{\epsilon_{max} - \epsilon_{min}} = \frac{\epsilon - 0.016921}{0.412598 - 0.016921} = \frac{\epsilon - 0.016921}{0.395677} \quad (11)$$

$$\epsilon_{EQ} = 0.395677\epsilon_N + 0.016921 \quad (12)$$

For all the desired strains, it is only necessary to provide these values of ϵ_{EQ} to the optimization algorithm and perform the simulation.

For the identification of the damage, the strain was analyzed in 10 points, located in distinct places of the beam; these points can be seen in Fig. 13a. Similarly, in the FEM we chose nodes located in positions equal to the points analyzed in the DIC. The strains observed at these points were normalized and transformed to the unit of measurement used by FEM. Table 6 shows these values.

By introducing these values in the SFO algorithm, the simulations were started in an attempt to identify the damage present in the beam. Eight simulations were performed, the results of which are presented in Table 7. The biological operators used in these simulations are the same as those

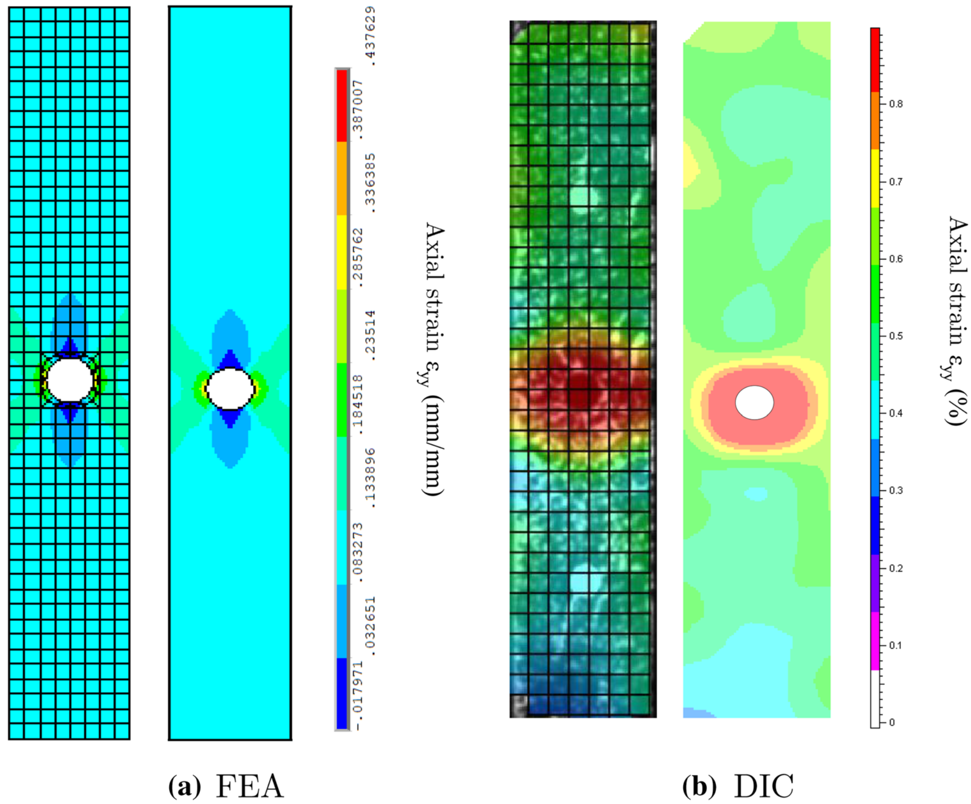

Fig. 13 Axial strain field obtained by **a** numerical analysis; and **b** digital image correlation before and after noise filtering

Table 6 Strain conversion found in DIC to the unit used by the FEM

Point	ϵ_{DIC}	ϵ_{NORM}	ϵ_{EQ} (FEM)
1	0.85	0.3778	0.1664
2	0.85	0.3778	0.1664
3	0.60	0.2667	0.1224
4	0.60	0.2667	0.1224
5	0.65	0.2889	0.1312
6	0.55	0.2444	0.1136
7	0.60	0.2667	0.1224
8	0.65	0.2889	0.1312
9	0.65	0.2889	0.1312
10	0.60	0.2667	0.1224

Table 7 Experimental damage detection resulting using DIC strains

	x (m)	y (m)	r (mm)
Objective	0.0150	0.1500	4.0000
Run 1	0.0151	0.1501	4.1647
Run 2	0.0148	0.1500	5.3387
Run 3	0.0148	0.1488	4.3245
Run 4	0.0151	0.1503	5.3713
Run 5	0.0231	0.1456	6.7453
Run 6	0.0151	0.1510	4.1241
Run 7	0.0147	0.1470	5.1213
Run 8	0.0148	0.1488	4.3245
Mean	0.0159	0.1490	4.9393
Deviation	0.0030	0.0099	0.8658

used to simulate the beam/plate in the previous section. These values can be verified in Table 4.

It was observed that in most of the results, the parameters related to the position of the damage (x, y), converged considerably to the real values. For the parameter referring to the dimension of the damage (r), although some results converge considerably to the real value, we can see a significant variability in its value, being thus the parameter more difficult to be detected. It is important to say here that even if there is a deviation in the radius, it is relatively small and the region in which the damage is found within the beam/plate is practically the same, thus reducing the area to be evaluated in a maintenance process. Thus, we show again the efficiency of SFO. All this can be verified also by observing the values of the deviations, in which the deviation of r is considerably greater than the deviations of x and y.

It is possible to verify that among the presented results, there is one (Run 5) that is remarkably different from the objective result; this could have occurred due to the problem not being minimized properly; in this way, it may be necessary to increase the values of the biological operators flowers and/or generations, causing the problem to be minimized properly. However, as a consequence of this,

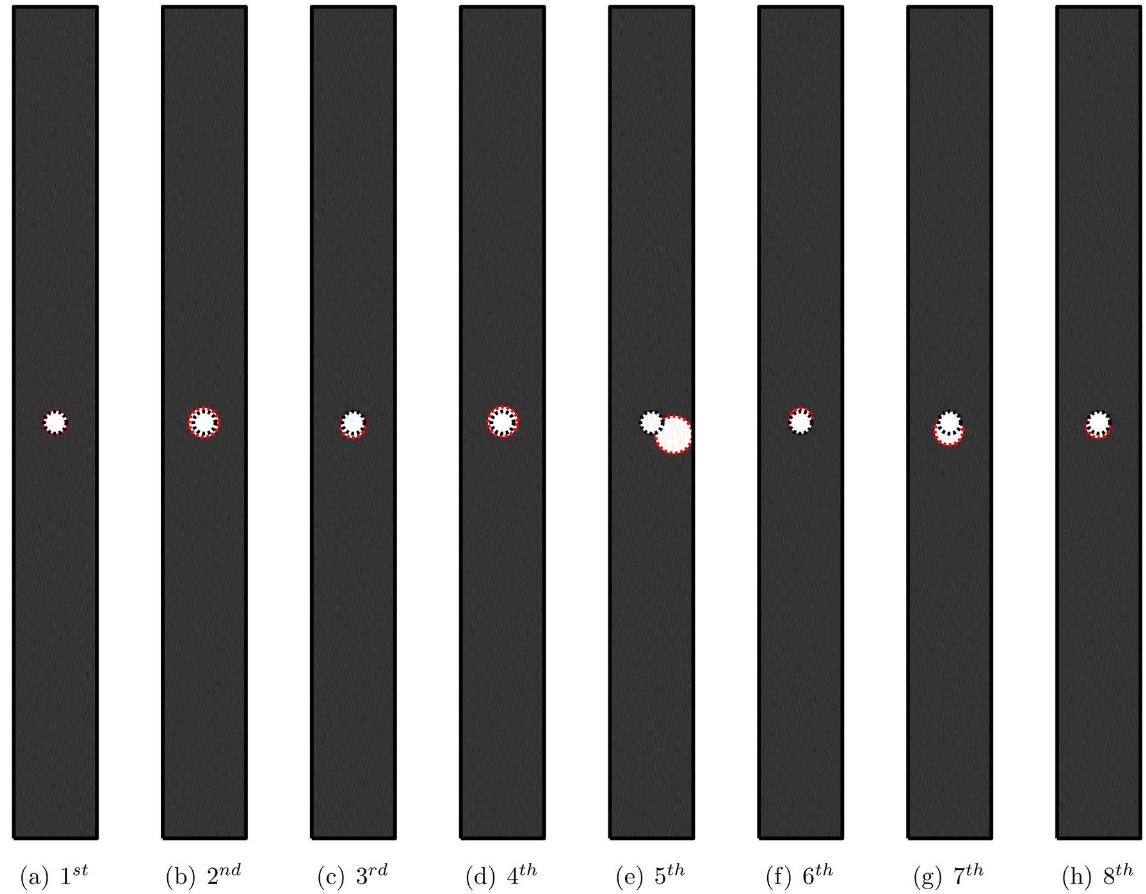

Fig. 14 Damage identification results using experimental data, all separated cases (legend: red dotted line; identified damages black dotted line; real damage) (color figure online)

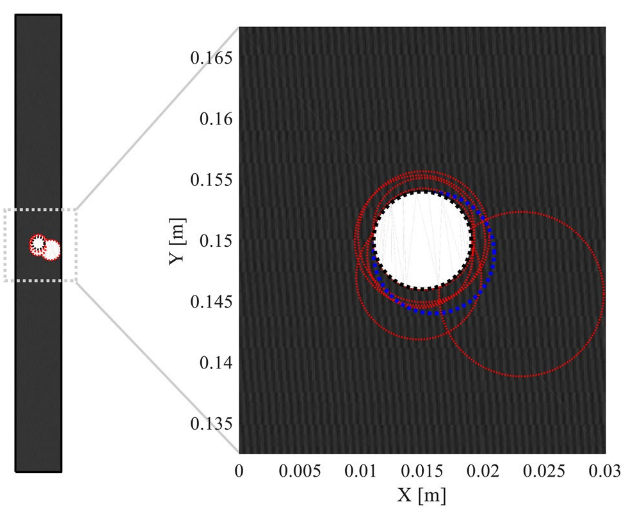

Fig. 15 General experimental results of the damage identification using SFO and DIC (legend: red dotted line; identified damages black dotted line; real damage blue dotted line; mean) (color figure online)

there is a need for more computational time and effort. Figures 14 and 15 show the results presented in Table 7, where you can easily see what was reported above.

Now, by making a comparison between the experimental results (Table 7) and the computational results (presented in Table 5 - Damage 1), both depicting the same case (beam with a hole in the center), it is noted that computational results are more accurate, since their parameters approximate the real values more accurately. However, it is important to emphasize that because these are experimental results, the results presented in Table 7 are satisfactory, since a good part of them approached the actual damage in the body of evidence. Certainly, evaluating the methodology used in more complex structures would be fundamental. However, this study is limited by the optical test laboratory equipment. In a promising future, the correlation of images will reach a level of being portable and in increasingly smaller equipment.

5 Conclusion

Despite the need to make some adaptations, the effectiveness of the SFO algorithm was verified when applied to the static analysis, since the simulations were performed without interruptions or errors of operation.

The SFO algorithm obtained a good behavior in all the simulations carried out, so it is possible to prove an appropriate operation both in the application of the plate and in the application of the beam. As for the application of the SFO algorithm in the detection of damages, more specifically in the case of circular holes, a satisfactory performance is observed regardless of its position and dimension, since for all the simulations values were very close to the ones parameters.

Although the method achieves satisfactory results, related to the parameters of the damages, a variation in its efficiency is noticed, this is due to the dependence of the results in relation to the biological operators. Since using larger amounts of plants and / or generations, there is a decrease in the standard deviation; that is, more accurate results are obtained, but a higher computational cost and a longer simulation time are required.

Turning now to the experimental part, it was found that the results obtained through the DIC technique are valid, since, to a certain extent, they represented well the damage in the body of evidence. However, these results can be improved in two different ways: the first increasing the number of simulations and thus improving the mean value of the parameters to be identified and the second increasing the values of the biological operators (flowers and generations) thus increasing the possibility of properly minimizing the problem, thus generating more precise results. However, in these cases there is also a need for more time in the damage identification process and for the second case there is also a need for higher computational costs. Despite all that has been said above, it can be ensured that the application of the DIC technique achieved the desired success, since much of the results represented the actual damage in a considerable way.

The present study has shown the potential of DIC for SHM of composite structures. It is revealed as an efficient methodology to identify possible damage in laminates with geometric discontinuities. It is still a challenge though to accurately identify internal damage such as delamination.

With this, it can be said that this method has great potential to be applied in several engineering cases: firstly, due to the fact that the method produces relevant results. But mainly because of the practical advantages of the method, since it can be applied in an uninterrupted way by monitoring the structure continuously, it requires little time to carry out the inspection, the results are constant being dependent almost only on the adjustment and the quality of the used instruments and also has low cost with instrumentation and operation. In this way, when compared to conventional methods of damage identification, the method used in this work becomes more practical and efficient in most engineering applications.

In summary, the SFO algorithm behaved appropriately in all cases where it was applied, generating relevant results in all of them. In the same way, the experiment performed using the DIC technique was also successful, generating mostly relevant results, leading the SFO algorithm to identify damages similar to the actual damage in the test body.

Acknowledgements The authors would like to acknowledge the financial support from the Brazilian agency CNPq - Conselho Nacional de Desenvolvimento Cientıfico e Tecnolígico, CAPES - Coordenação de Aperfeiçoamento de Pessoal de Nıvel Superior and FAPEMIG - Fundação de Amparo à Pesquisa do Estado de Minas Gerais (APQ-00385-18). The authors would like to acknowledge also the Tutorial Education Program (PET)

Compliance with ethical standards

Conflict of interest The authors declare that they have no conflict of interest.

References

1. Balageas D, Fritzen C-P, Güemes A (2010) Structural health monitoring, vol 90. Wiley, Hoboken
2. Feng D, Feng MQ (2017) Experimental validation of cost-effective vision-based structural health monitoring. Mech Syst Signal Process 88:199–211
3. Gomes GF, Mendéz YAD, da Silva Lopes Alexandrino P, da Cunha SS Jr, Ancelotti AC Jr (2018) The use of intelligent computational tools for damage detection and identification with an emphasis on composites – A review. Compos Struct 196:44–54. https://doi.org/10.1016/j.compstruct.2018.05.002
4. Samir K, Brahim B, Capozucca R, Wahab MA (2018) Damage detection in cfrp composite beams based on vibration analysis using proper orthogonal decomposition method with radial basis functions and cuckoo search algorithm. Compos Struct 187:344–353
5. de Sousa BS, Gomes GF, Jorge AB, da Cunha SS Jr, Ancelotti AC Jr (2018) A modified topological sensitivity analysis extended to the design of composite multidirectional laminates structures. Compos Struct 200:729–746
6. de Souza A, Gomes GF, Peres EP, Isaías JC, Ancelotti AC (2019) A numerical-experimental evaluation of the fatigue strain limits of cfrp subjected to dynamic compression loads. Int J Adv Manuf Technol 103(1–4):219–237
7. Di Benedetto RM, Botelho EC, Gomes GF, Junqueira DM, Ancelotti Junior AC (2019) Impact energy absorption capability of thermoplastic commingled composites. Compos B Eng 176:107307
8. Bhudolia SK, Perrotey P, Joshi SC (2018) Mode i fracture toughness and fractographic investigation of carbon fibre composites with liquid methylmethacrylate thermoplastic matrix. Compos B Eng 134:246–253
9. Diniz CA, Cunha SS, Gomes GF, Ancelotti AC (2019) Optimization of the layers of composite materials from neural networks with tsai-wu failure criterion. J Fail Anal Prev 19(3):709–715

10. Gomes GF, Mendéz YAD, Simões S, da Cunha, Antônio CA (2018) A numerical-experimental study for structural damage detection in cfrp plates using remote vibration measurements. J Civ Struct Health Monit 8(1):33–47
11. da Silva P, Alexandrino L, Gomes GF, Jr Sebastião Simões C (2020) A robust optimization for damage detection using multiobjective genetic algorithm, neural network and fuzzy decision making. Inverse Prob Sci Eng 28(1):21–46
12. Heslehurst RB (2014) Defects and damage in composite materials and structures. CRC Press, Boca Raton
13. Gomes GF, de Almeida FA, da Silva Lopes Alexandrino P, da Cunha SS Jr, de Sousa BS, Ancelotti AC Jr (2018) A multiobjective sensor placement optimization for SHM systems considering Fisher information matrix and mode shape interpolation. Eng Comput 35(2):519–535. https://doi.org/10.1007/s00366-018-0613-7
14. Gopalakrishnan S, Ruzzene M, Hanagud S (2011) Computational techniques for damage detection, classification and quantification. In: Computational techniques for structural health monitoring. Springer, New York, pp 407–461
15. Yun-Lai Z, Maia Nuno MM, Sampaio Rui PC, Abdel WM (2017) Structural damage detection using transmissibility together with hierarchical clustering analysis and similarity measure. Struct Health Monit 16(6):711–731
16. Gillich G-R, Furdui H, Wahab MA, Korka Z-I (2019) A robust damage detection method based on multi-modal analysis in variable temperature conditions. Mech Syst Signal Process 115:361–379
17. Zhou Y-L, Wahab MA (2017) Cosine based and extended transmissibility damage indicators for structural damage detection. Eng Struct 141:175–183
18. Zhou Y-L, Maia NMM, Wahab MA (2018) Damage detection using transmissibility compressed by principal component analysis enhanced with distance measure. J Vib Control 24(10):2001–2019
19. Khatir S, Wahab MA, Boutchicha D, Khatir T (2019) Structural health monitoring using modal strain energy damage indicator coupled with teaching-learning-based optimization algorithm and isogoemetric analysis. J Sound Vib 448:230–246
20. Ribeiro Junior RF, de Almeida FA, Gomes GF (2020) Fault classification in three-phase motors based on vibration signal analysis and artificial neural networks. Neural Comput Appl. https://doi.org/10.1007/s00521-020-04868-w
21. Barbosa LCM, Santos M, Oliveira TLL, Gomes GF, Ancelotti AC Jr (2019) Effects of moisture absorption on mechanical and viscoelastic properties in liquid thermoplastic resin/carbon fiber composites. Polymer Eng Sci 59(11):2185–2194
22. Barbosa LCM, Gomes G, Junior ACA (2019) Prediction of temperature-frequency-dependent mechanical properties of composites based on thermoplastic liquid resin reinforced with carbon fibers using artificial neural networks. Int J Adv Manuf Technol 105(5–6):2543–2556
23. Chandarana N, Sanchez D, Soutis C, Gresil M (2017) Early damage detection in composites during fabrication and mechanical testing. Materials 10(7):685
24. Kessler SS, Mark Spearing S, Atalla MJ, Cesnik CES, Soutis C (2002) Damage detection in composite materials using frequency response methods. Compos B Eng 33(1):87–95
25. Cantwell WJ, Morton J (1992) The significance of damage and defects and their detection in composite materials: a review. J Strain Anal Eng Des 27(1):29–42
26. Pearson MR, Eaton MJ, Featherston CA, Holford KM, Pullin R (2011) Impact damage detection and assessment in composite panels using macro fibre composites transducers. J Phys Conf Ser 305:012049
27. Gomes GF, Pereira JVP (2020) Sensor placement optimization and damage identification in a fuselage structure using inverse modal problem and firefly algorithm. Evol Intell 1–21
28. François H, Jean-Noël P, Stéphane R (2015) Evaluating damage with digital image correlation: C. applications to composite materials. In: Handbook of damage mechanics: nano to macro scale for materials and structures, pp 1301–1322
29. Caminero MA, Lopez-Pedrosa M, Pinna C, Soutis C (2014) Damage assessment of composite structures using digital image correlation. Appl Compos Mater 21(1):91–106
30. Fister Jr I, Yang X-S, Fister I, Brest J, Fister D (2013) A brief review of nature-inspired algorithms for optimization. arXiv preprint arXiv:1307.4186
31. Yang X-S, Xingshi H (2016) Nature-inspired optimization algorithms in engineering: overview and applications. Nature-inspired computation in engineering. Springer, New York, pp 1–20
32. Gomes GF, Mendez YAD, Alexandrino Patrícia da Silva L, da Cunha SS, Ancelotti AC (2018) A review of vibration based inverse methods for damage detection and identification in mechanical structures using optimization algorithms and ann.In: Archives of computational methods in engineering, pp 1–15
33. Zenzen R, Belaidi I, Khatir S, Wahab MA (2018) A damage identification technique for beam-like and truss structures based on frf and bat algorithm. Comptes Rendus Mécanique 346(12):1253–1266
34. Tran-Ngoc H, De Samir Khatir G, Roeck T, Bui-Tien LN-N, Wahab MA (2018) Model updating for nam o bridge using particle swarm optimization algorithm and genetic algorithm. Sensors 18(12):4131
35. Khatir S, Abdel Wahab M (2019) Fast simulations for solving fracture mechanics inverse problems using pod-rbf xiga and jaya algorithm. Eng Fract Mech 205:285–300
36. Samir Khatir and Magd Abdel Wahab (2019) A computational approach for crack identification in plate structures using xfem, xiga, pso and jaya algorithm. Theor Appl Fract Mech 103:102240
37. Gomes GF, Simões S, da Cunha A, Ancelotti C (2019) A sunflower optimization (sfo) algorithm applied to damage identification on laminated composite plates. Eng Comput 35(2):619–626
38. Caminero MA, Pavlopoulou S, Lpez-Pedrosa M, Nicolaisson BG, Pinna C, Soutis C (2012) Digital image correlation analysis applied to monitor damage evolution of composite plates with stress concentrations and bonded patch repairs. In: Proceedings of the 15th European conference on composite materials, Venice, Italy, pp 24–28
39. Memmolo V, Monaco E, Boffa ND, Maio L, Ricci F (2018) Guided wave propagation and scattering for structural health monitoring of stiffened composites. Compos Struct 184:568–580
40. Zuo H, Yang Z, Xu C, Tian S, Chen X (2018) Damage identification for plate-like structures using ultrasonic guided wave based on improved MUSIC method. Compos Struct 203:164–171. https://doi.org/10.1016/j.compstruct.2018.06.100
41. Yang Z-B, Radzienski M, Kudela P, Ostachowicz W (2017) Damage detection in beam-like composite structures via chebyshev pseudo spectral modal curvature. Compos Struct 168:1–12
42. Xingwu Z, Gao Robert X, Ruqiang Y, Xuefeng C, Chuang S, Zhibo Y (2016) Multivariable wavelet finite element-based vibration model for quantitative crack identification by using particle swarm optimization. J Sound Vib 375:200–216
43. Yang Z-B, Radzienski M, Kudela P, Ostachowicz W (2017) Fourier spectral-based modal curvature analysis and its application to damage detection in beams. Mech Syst Signal Process 84:763–781
44. Stepinski T, Uhl T, Staszewski W (2013) Advanced structural damage detection: from theory to engineering applications. Wiley, Hoboken
45. Worden K, Staszewski W, Manson G, Ruotulo A, Surace C (2008) Optimization techniques for damage detection. In: Encyclopedia of structural health monitoring. Wiley. https://doi.org/10.1002/9780470061626.shm057
46. Rytter A (1993) Vibrational based inspection of civil engineering structures. PhD thesis, Dept. of Building Technology and Structural Engineering, Aalborg University

47. Shi D, Xiao X (2018) An enhanced continuum damage mechanics model for crash simulation of composites. Compos Struct 185:774–785
48. Soriano A, Díaz J (2018) Failure analysis of variable stiffness composite plates using continuum damage mechanics models. Compos Struct 184:1071–1080
49. Ben Sghaier R, Majed N, Ben Dali H, Fathallah R (2017) High cycle fatigue prediction of glass fiber-reinforced epoxy composites: reliability study. Int J Adv Manuf Technol 92(9–12):4399–4413
50. Sundararaman S, Adams DE, Rigas EJ (2005) Structural damage identification in homogeneous and heterogeneous structures using beamforming. Struct Health Monit 4(2):171–190
51. Reddy JN, Miravete A (2018) Practical analysis of composite laminates. CRC Press, Boca Raton
52. Sridharan S (2008) Delamination behaviour of composites. Elsevier, Amsterdam
53. Niemann H, Morlier J, Shahdin A, Gourinat Y (2010) Damage localization using experimental modal parameters and topology optimization. Mech Syst Signal Process 24(3):636–652
54. Montalvao D, Maia NMM, Ribeiro AMR (2006) A review of vibration-based structural health monitoring with special emphasis on composite materials. Shock Vib Digest 38(4):295–324
55. Zou Y, Tong LPSG, Steven GP (2000) Vibration-based model-dependent damage (delamination) identification and health monitoring for composite structures—a review. J Sound Vib 230(2):357–378
56. Liu PF, Zheng JY (2010) Recent developments on damage modeling and finite element analysis for composite laminates: A review. Mater Des 31(8):3825–3834
57. Chao X, Qi L, Cheng J, Tian W, Zhang S, Li H (2018) Numerical evaluation of the effect of pores on effective elastic properties of carbon/carbon composites. Compos Struct 196:108–116
58. Drach B, Tsukrov I, Trofimov A, Gross T, Drach A (2018) Comparison of stress-based failure criteria for prediction of curing induced damage in 3d woven composites. Compos Struct 189:366–377
59. Sokolnikoff IS (1956) Mathematical theory of elasticity. McGraw-Hill Book Company, New York
60. Malvern LE (1969) Introduction to the mechanics of a continuous medium (No. Monograph)
61. Ugural Ansel C, Fenster Saul K (2011) Advanced mechanics of materials and applied elasticity. Pearson Education, London
62. Pilkey Walter D, Pilkey Deborah F (2008) Peterson's stress concentration factors. Wiley, Hoboken
63. Carlos AJA, Claudio PL, Marcelo BE, Dennis R (2010) Use of the mar-lin criteria to determine the influence of porosity on the iosipescu and short beam shear properties in carbon fiber polymer matrix composites. Mater Res 13(1):63–69
64. Ye L, Afaghi-Khatibi A, Lawcock G, Mai Y-W (1998) Effect of fibre/matrix adhesion on residual strength of notched composite laminates. Compos A Appl Sci Manuf 29(12):1525–1533
65. Tan Seng C (1994) Stress concentrations in laminated composites. CRC Press, Boca Raton
66. Chu TC, Ranson WF, Sutton MA (1985) Applications of digital-image-correlation techniques to experimental mechanics. Exp Mech 25(3):232–244
67. Orell O, Vuorinen J, Jokinen J, Kettunen H, Hytönen P, Turunen J, Kanerva M (2018) Characterization of elastic constants of anisotropic composites in compression using digital image correlation. Compos Struct 185:176–185
68. Tekieli M, De Santis S, de Felice G, Kwiecień A, Roscini F (2017) Application of digital image correlation to composite reinforcements testing. Compos Struct 160:670–688
69. Peters WH, Ranson WF (1982) Digital imaging techniques in experimental stress analysis. Opt Eng 21(3):213427
70. Sutton MA, Wolters WJ, Peters WH, Ranson WF, McNeill SR (1983) Determination of displacements using an improved digital correlation method. Image Vis Comput 1(3):133–139
71. Beberniss TJ, Ehrhardt DA (2017) High-speed 3d digital image correlation vibration measurement: Recent advancements and noted limitations. Mech Syst Signal Process 86:35–48
72. Crammond G, Boyd SW, Dulieu-Barton JM (2013) Speckle pattern quality assessment for digital image correlation. Opt Lasers Eng 51(12):1368–1378
73. Johanson K, Harper LT, Johnson MS, Warrior NA (2015) Heterogeneity of discontinuous carbon fibre composites: damage initiation captured by digital image correlation. Compos A Appl Sci Manuf 68:304–312
74. Speranzini E, Agnetti S (2014) The technique of digital image correlation to identify defects in glass structures. Struct Control Health Monit 21(6):1015–1029
75. Yoneyama S, Murasawa G (2009) Digital image correlation. Exp Mech 207
76. Gomes GF, da Cunha SS Jr, da Silva Lopes Alexandrino P, Silva de Sousa B, Ancelotti AC Jr (2018) Sensor placement optimization applied to laminated composite plates under vibration. Struct Multi Optim 58(5):2099–2118. https://doi.org/10.1007/s00158-018-2024-1
77. Khatir S, Dekemele K, Loccufier M, Khatir T, Wahab MA (2018) Crack identification method in beam-like structures using changes in experimentally measured frequencies and particle swarm optimization. Comptes Rendus Mécanique. 346(2):110–120
78. Braun CE, Chiwiacowsky LD, Gomez AT (2015) Variations of ant colony optimization for the solution of the structural damage identification problem. Procedia Comput Sci 51:875–884
79. Kim N-I, Kim S, Lee J (2019) Vibration-based damage detection of planar and space trusses using differential evolution algorithm. Appl Acoust 148:308–321
80. Bayraktar Z, Komurcu M, Bossard JA, Werner DH (2013) The wind driven optimization technique and its application in electromagnetics. IEEE Trans Antennas Propag 61(5):2745–2757
81. Yang X-S (2012) Flower pollination algorithm for global optimization. In: International conference on unconventional computing and natural computation. Springer, New York, pp 240–249
82. Richards SHANEA (1997) Completed richardson extrapolation in space and time. Commun Numer Methods Eng 13(7):573–582
83. Robert Frank G (2007) Sensor placement optimization under uncertainty for structural health monitoring systems of hot aerospace structures. PhD thesis, Citeseer
84. Ray-Chaudhuri S, Chawla K (2018) Stress and strain concentration factors in orthotropic composites with hole under uniaxial tension. Curved Layer Struct 5(1):213–231
85. Perumal L, Tso CP, Leng LT (2016) Analysis of thin plates with holes by using exact geometrical representation within xfem. J Adv Res 7(3):445–452
86. Taynara Incerti de Paula, Guilherme FG, José Henrique de Freitas G, Anderson Paulo de Paiva (2019) A mixture design of experiments approach for genetic algorithm tuning applied to multi-objective optimization. In: World Congress on Global Optimization. Springer, New York, pp 600–610
87. Qais MH, Hasanien HM, Alghuwainem S (2019) Identification of electrical parameters for three-diode photovoltaic model using analytical and sunflower optimization algorithm. Appl Energy 250:109–117
88. Shaheen MAM, Hasanien HM, Mekhamer SF, Talaat HEA (2019) Optimal power flow of power systems including distributed generation units using sunflower optimization algorithm. IEEE Access 7:109289–109300